Renewable Energy 222 (2024) 119874

Contents lists available at ScienceDirect

Renewable Energy

journal homepage: www.elsevier.com/locate/renene

A novel supercritical carbon dioxide combined cycle fueled by biomass: Thermodynamic assessment

Shayan Sharafi laleh [a], Seyed Hamed Fatemi Alavi [a], Saeed Soltani [b,*], S.M.S. Mahmoudi [a,**], Marc A. Rosen [c]

[a] *Faculty of Mechanical Engineering, University of Tabriz, 16471, Tabriz, Iran*
[b] *Faculty of Engineering and Natural Sciences, Antalya Bilim University, 07190, Antalya, Turkey*
[c] *Faculty of Engineering and Applied Science, University of Ontario Institute of Technology, 2000 Simcoe Street North, Oshawa, Ontario, L1G 0C5, Canada*

ARTICLE INFO

Keywords:
Combined cycle
Gasification
Biomass
Equilibrium model
Recompression supercritical carbon dioxide
Energy analysis

ABSTRACT

As a carbon-neutral type of renewable energy, biomass is beneficial for reducing carbon emissions in the electricity sector. A biomass gasification process integrated with a combined cycle is proposed here. Wood is chosen as the fuel and air as the gasifying agent. A supercritical carbon dioxide (SCO_2) power cycle with recompression is selected for the recovery of waste heat from the combustion chamber. The net power output is considered to be 1 MW for the combined cycle in the investigation of component ratings and biomass feed rate. For a comprehensive thermodynamic analysis of this combined cycle, we examine three key parameters: gas turbine inlet temperature (1200–1400 K), topping cycle pressure ratio (5-10) and CO_2 turbine inlet temperature (600–700 K). The maximum energy efficiency is achieved for the system at a specific pressure ratio and CO_2 turbine inlet temperature. The energy efficiency rises with gas turbine inlet temperature, which reduces biomass consumption (at a fixed net power output). The CO_2 emission rate to the environment is examined for various parameters; it is observed to decrease as biomass consumption decreases and to take on a value of 0.254 kg/s at an optimized state.

1. Introduction

CO_2 emissions have reached concerning levels in recent years, and a large amount of CO_2 is emitted from fossil fuel-based power generation plants, which account for approximately 40 % of global CO_2 emissions [1]. Global warming and other ecosystem damage have led to growing interest in renewable energy. Using biomass as a fuel is one way to lower CO_2 emissions and move towards sustainable energy. Biomass is a widely available energy resource, and can be derived from agriculture, forestry, fishery and aquaculture industries, and in particular from algae and waste [2]. When considering economic and environmental characteristics of energy sources together, biomass is often considered advantageous, particularly because of its wide distribution and low cost [3, 4]. Unlike fossil fuels, biomass is significantly easier and faster to replace by methods like artificial forestry. However, a disadvantages of plants that use biomass as fuel for power generation is their low overall efficiency (from 15 % to 30 %, depending on plant size) compared to plants utilizing fossil fuels like natural gas [5,6]. Gas turbines require constant cleaning and maintenance to operate efficiently, involving the utilization of costly gas cleaning systems after the gasification process [7–9]. These technical issues need further optimization efforts and analyses (thermodynamic and economic) [7,10,11]. An option to overcome this problem is to use an externally fired gas turbine (EFGT) driven by biomass [8,12]. EFGTs can be applied in combined cycles (e.g., plants with Brayton and Rankine cycles as topping and bottoming cycles, respectively) [13], in electricity and heating systems [14,15], and in system hybridized via inclusion of solar thermal energy or other forms of renewable energy [16,17].

An EFGT using biomass as a fuel was investigated by Soltani et al. [18]. In that study, a conventional Rankine steam cycle constitutes the bottoming cycle and is applied for recovery of waste heat. An advantageous waste heat recovery method for the gas turbine exhaust is through a Rankine steam cycle, which permits good heat extraction from the gas turbine exhaust at high energy efficiency; nonetheless, the properties of water lead to more sophisticated components which can increase the total capital cost of the system. Although equipment design and plant layout complexity are reasonable for high capacity gas

* Corresponding author.
** Corresponding author.
E-mail addresses: soltani929@gmail.com, saeed.soltani@antalya.edu.tr (S. Soltani), s_mahmoudi@tabrizu.ac.ir (S.M.S. Mahmoudi).

https://doi.org/10.1016/j.renene.2023.119874
Received 17 January 2023; Received in revised form 16 December 2023; Accepted 20 December 2023
Available online 21 December 2023

Nomenclature

A	Surface area
CETD	Cold end temperature difference of heat exchanger
CTIT	Carbon dioxide turbine inlet temperature
EFGT	Externally fired gas turbine
EFGTRC	Externally fired gas turbine combined with recompression CO_2
ε	Recuperator effectiveness
GA	Gasifier
GT	Gas turbine
h	Specific enthalpy
h_f	Specific enthalpy of formation
HE	Heat exchanger
HTR	High temperature recuperator
HHV	Lower heating value
K	Equilibrium constant
LHV	Lower heating value
LTR	Low temperature recuperator
m	Molar quantity of oxygen per kmol of wood in gasifier
N	Molar quantity of any substance per kmol of mixed gas
MC	Moisture content per mole of biomass
P_i	Pressure at state i
PC	Precooler
PRc	CO_2 recompression cycle pressure ratio
Δp	Pressure drop
R_p	Pressure ratio
REC	Recompression compressor
$\bar{r}$	Universal gas constant
s	Specific entropy
T_i	Temperature at state i
TIT	Gas turbine inlet temperature
w	Amount of water per kmol of paper
W	Work
x	Stream split ratio
X	Number of moles

Subscripts

B	producer gas after gasification of biomass
c	carbon dioxide
C	compressor
CC	combustion chamber
g	product gas
G	gasifier
GT	gas turbine
HE	heat exchanger
in	input
i	index for thermodynamic state point
out	outlet

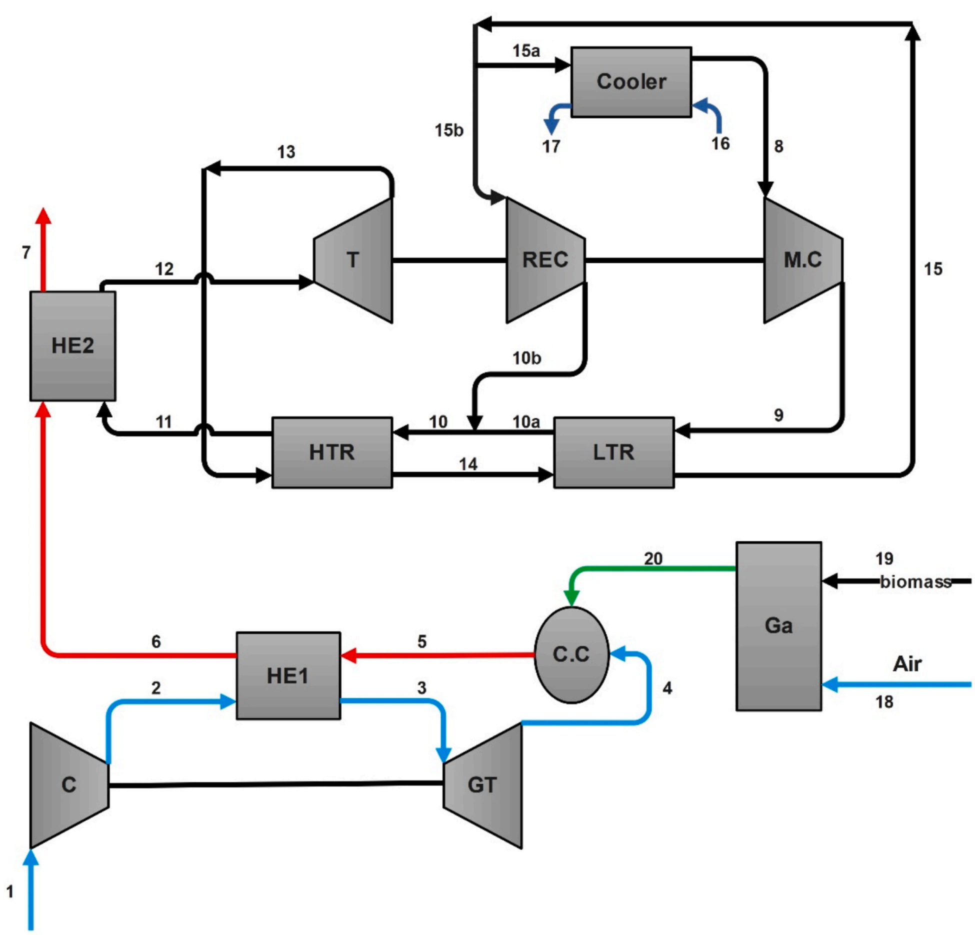

Fig. 1. Externally fired gas turbine combined with SCO_2 recompression cycle.

turbines, they are not acceptable for internal combustion engines and/or gas turbine plants [19,20].

These issues can be addressed via SCO_2 cycles. By working at high cycle pressures throughout, the working fluid has a high density and correspondingly utilizes smaller equipment, resulting in lower capital costs and environmental impact [21–23]. SCO_2 Brayton cycles have been investigated for various applications recently, including advanced nuclear reactors, geothermal and solar energy, high temperature fuel cells, and waste heat recovery from gas turbines. All of these help address ecological and environmental pressures and problems of fossil energy shortages. Numerous SCO_2 Brayton cycle layouts have been studied and their performances as bottoming cycles examined [19,21].

A combined cycle power plant typically offers higher efficiency compared to a semi-closed cycle. This is because a combined cycle integrates gas and CO_2 turbines, utilizing waste heat from the gas turbine to generate additional electricity in the CO_2 gas turbine. This dual-cycle configuration enhances overall efficiency and allows for better utilization of energy resources. In the present work, an EFGT is coupled with a recompression SCO_2 Brayton cycle to examine the efficiency and thermodynamic characteristics of this novel system, and to examine the potential use of biomass fuel. The novelty of the present study lies in its examination of the utilization of a recompression Brayton SCO_2 cycle and its characteristics as a bottoming cycle for an externally fired gas turbine using biomass as the only fuel. This combined cycle is feasible and relatively straightforward to construct and maintain, in part because of the characteristics of the SCO_2 recompression Brayton cycle, which is used as a bottoming cycle. The proposed plant has smaller and simpler equipment and the EFGT uses a clean working fluid in the gas turbine. These characteristics can help in selecting the proper components for the plant.

2. System description

The considered externally fired gas turbine combined with SCO_2 recompression cycle (EFGTRC) is shown in Fig. 1. Key components of the EFGTRC include the heat exchangers, which provide the required heat from hot product gases to the working fluids to generate electricity.

The combined cycle includes bottoming and topping cycles. In this paper, the intended topping cycle is similar to that investigated by Soltani et al. [18]. The required agent (air) for the gasifier is provided from the environment. Datta et al. [8] use a compressor to provide the required air for the gasifier. Based on wide accessibility and reasonably good LHV, wood is considered as the fuel here.

An important aspect of using an externally fired layout for the gas turbine is that the combustion gases for biomass based fuels are not as clean as other fuels such as natural gas. So utilizing this layout may be important as the gas turbines are expensive and hard to maintain.

It is seen in Fig. 1 that the compressed air reaches the gas turbine inlet temperature (point 3) via heating with the hot gases that pass through heat exchanger 1 (HE1) at point 6. These exiting hot gases then heat SCO_2 to the required temperature in heat exchanger 2 (HE2) at point 7. In the topping cycle, compressed air is heated in HE1 and utilized in the gas turbine for power generation instead of using the exiting hot gases from the combustion chamber directly. According to some studies, ceramic heat exchangers are suitable for operation at high temperatures like 1500 K, but usually for steel heat exchangers a reasonable working temperature is limited to 1050–1100 K. For higher temperatures like 1400 K an advanced heat exchanger is required [24]. The temperature difference in HE1 is the key parameter to select the system's bottoming cycle layout. If the temperature difference is too low, the exiting hot gases from HE1 are colder and not suitable to permit a supercritical closed Brayton cycle as the bottoming cycle, although the topping cycle's performance would be better.

A recompression Brayton cycle forms the bottoming cycle. It uses CO_2 as a working fluid. At the LTR exit (point 15), the hot CO_2 stream is split. One of the separated streams undergoes precooling and compression (point 15a and 8), and the other stream is compressed in the recompressing compressor (point 10b). After merging at point 10, the CO_2 stream is preheated by the exiting stream from the turbine at the HTR (point 11). Before entering the turbine, the CO_2 stream reaches the CO_2 turbine inlet temperature (CTIT) of the heat exchanger (HE2) using gases exiting the combustion chamber (point 12). The maximum temperature increase for the precooler (PC) is taken to be 10 K, a limit to alleviate environmental issues related to thermal pollution [25]. At point 10, the two merging streams (10a and 10b) are considered to be at equal temperatures to achieve the optimum value for the stream split ratio x [26]. Note that the SCO_2 recompression cycle operates over a small temperature range because of the utilization of two recuperators, which raise the CO_2 temperature before it enters HE2.

System parameters are listed in Table 1 with their values, while assumptions invoked in the analyses follow.

1. The cycles operate at steady state.
2. Heat transfer with the ambient space can be neglected, except in precoolers [21].
3. Pressure losses are negligible in tubes and heat exchangers.
4. Cooling water input to the precooler is at ambient temperature and pressure.

3. Energy analysis

The thermodynamic analysis methodology used here follows that of similar studies [8,27,28]. The gasifier is the most significant component, so particular attention is paid to it.

The first law of thermodynamics is applied in order to assess the performance of the cogeneration system. The system's first law efficiency, often known as energy efficiency, can be expressed as:

$$\text{Energy efficiency} = \frac{\dot{W}_{net}}{\dot{m}_{biomass}\mathrm{LHV}_{biomass}} \tag{1}$$

3.1. Gasifier analysis

All reactions that take place in the gasifier are assumed to be in thermodynamic equilibrium. Before leaving the gasifier, we anticipate that the products of pyrolysis combust and reach equilibrium in the reduction zone [27–29]. Therefore, the downdraft gasifier can be modeled using an equilibrium model. The respective reactions follow:

$$C + CO_2 \leftrightarrow 2CO \tag{2}$$

$$C + H_2O \leftrightarrow CO + H_2 \tag{3}$$

$$C + 2H_2 \leftrightarrow CH_4 \tag{4}$$

Table 1
System parameters and their values [8,19,21].

Parameter	Value
Net output power, P_{net}	1 MW
Biomass moisture content by mass	20 %
Ambient pressure	101.325 kPa
Compressor isentropic efficiency for topping cycle	87 %
Gas turbine isentropic efficiency	89 %
Compressor pressure ratio for topping cycle	7
CETD for HE2	20 K
SCO_2 minimum pressure	7.4 MPa
SCO_2 maximum pressure	20 MPa
SCO_2 minimum temperature	32 °C
Turbine isentropic efficiency for bottoming cycle	90 %
Compressor isentropic efficiency for bottoming cycle	85 %
Recuperator effectiveness	86 %
CTIT	650 K
TIT	1200–1400 K

$$CO + H_2O \leftrightarrow CO_2 + H_2 \tag{5}$$

For methane formation (Eq. (4)), the equilibrium constant is:

$$K_1 = \frac{P_{CH_4}}{(P_{H_2})^2} \tag{6}$$

Methane will be formed when carbon and hydrogen combine. This reaction, which releases heat, is known as hydrogenolysis or, more frequently, the carbon-hydrogen reaction.

The equilibrium constant for the shift reaction (Eq. (5)) is:

$$K_2 = \frac{P_{CO_2}P_{H_2}}{P_{CO}P_{H2O}} \tag{7}$$

The shift reaction is the process by which carbon monoxide reacts with water to produce carbon dioxide and hydrogen. The reaction equilibrium moves to the right in Eq. (5) and supports the creation of the H_2 and CO_2 products at lower temperatures since the reaction also releases heat.

For a gasification process, the major chemical reactions affecting the heating value of the products are those involving carbon. The typical global gasification equation is [18]:

$$CH_{1.44}O_{0.66} + wH_2O + m(O_2 + 3.76N_2) \rightarrow n_1H_2 + n_2CO + n_3CO_2 + n_4H_2O + n_5CH_4 + n_6N_2 \tag{8}$$

Here, w is assigned to the quantity of water per kmol of wood and m to the quantity of oxygen per kmol of wood entering the gasifier from the environment, while n_1, n_2, n_3, n_4, n_5 and n_6 are the constituent coefficients for the obtained biofuel. Also, MC denotes the moisture content per mole of wood, expressible as follows:

$$MC = \frac{18w}{24 + 18w} \tag{9}$$

Therefore,

$$w = \frac{24MC}{18(1 - MC)} \tag{10}$$

The value of w is fixed because MC is assumed constant. Balancing the main process components (hydrogen, oxygen and carbon) in the reaction (Eq. (8)) provides the values of n_1 through n_6. By obtaining the values of the biofuel coefficient we can calculate the values of the equilibrium constants for methane formation and the water–gas shift reactions [27,29,30]. For methane formation (Eq. (6)) and the shift reaction (Eq. (7)), the respective equilibrium constants are

$$K_1 = \frac{n_5}{(n_1)^2} \tag{11}$$

and

$$K_2 = \frac{n_3 n_1}{n_2 n_4} \tag{12}$$

The gasification temperature (T_g) is obtained via an energy balance when no heat loss is assumed for the gasifier:

$$h^\circ fwood + wh^\circ fH2O = n_1 (h^\circ fH2 + \Delta h) + n_2 (h^\circ fCO + \Delta h) + n_3 (h^\circ fCO2 + \Delta h) + n_4 (h^\circ fH2O + \Delta h) + n_5 (h^\circ fCH4 + \Delta h) + n_6 (h^\circ fN2 + \Delta h) \tag{13}$$

Here, h°fwood, h°fH2O, h°fH2, h°fCO, h°fCO2, h°fH2O, h°fCH4 and h°fN2are the enthalpies of formation of the gasification products. The fuel's heating value is provided by the enthalpy of formation of wood [27]. Utilizing the values of the biofuel coefficients and T_g for Eq. (13) simultaneously provides the composition and temperature of the biofuel. Table 2 compares the biofuel composition for the present results with other studies, considering T_g = 800 °C and a 20 % MC. The hydrogen percentage calculated here is 18.2 % higher than that for the experiment by Alauddin [31],while the experimental percentage of carbon monoxide obtained here exceeds by 22.7 % that of Alauddin. These two components significantly affect the caloric value of the biofuel and have a large impact on biomass usage. The composition of the biomass (wood) by mass is reported to be 50 % carbon, 6 % hydrogen, 0 % nitrogen, 0 % sulfur, 44 % oxygen, and 0 % ash, and the biomass has a higher heating value (HHV) of 449,568 kJ/kmol[18].

Table 2
Comparison of experimental and model constituent breakdowns (in %) for wood with a moisture content of 20 % at a gasification temperature of 800 °C.

Constituent	Zainal equilibrium model [27]	Experiment [31]	Present study
Hydrogen	21.06	15.23	18.01
Methane	0.64	1.58	0.68
Carbon monoxide	19.61	23.04	18.77
Carbon dioxide	12.01	16.42	13.84
Oxygen	0.00	1.42	0.00
Nitrogen	46.68	42.31	48.7

To further evaluate the viability of the simulated gasification process with wood, the cold gas efficiency of using biofuel is taken to consideration. The cold gas efficiency can be expressed as [27]:

$$\text{Cold gas efficiency} = \frac{Biofuel\ LHV \left(\frac{kJ}{Nm^3}\right) \times Gas\ production\ rate \left(\frac{Nm^3}{kg}\right)}{Biomass\ LHV \left(\frac{kJ}{kg}\right)} \tag{14}$$

In this study, a cold gas efficiency of about 74.6 % is achieved.

3.2. Analysis of heat exchangers

In the present study, heat exchangers have a vital role on the system's overall performance, as HE1 provides heat needed for the compressed air prior to its input to the gas turbine and HE2 uses the exiting hot gases for heat recovery. For a better understanding of this particular component, we consider the cold end temperature difference (CETD) of the heat exchangers to be fixed. Doing so helps in monitoring the values of biomass consumption and exiting temperature of hot gases. Expressions to model the heat exchangers are shown in Table 3 and the effect of CETD for HE1 is examined in the results and discussion section.

As the present work has numerous similarities in the case of the topping cycle and its components, the combustion chamber of the system is not discussed here further, as it has been described by Soltani et al. [18].

Table 3
Thermodynamic model of EFGTRC system.

Component	Expression
C	$W_C = 4.76n_{Air} (h_2 - h_1)$
GT	$W_{GT} = 4.76n_{Air} (h_3 - h_4)$
HE1	$4.76n_{Air} (h_3 - h_4) = X_G (h_5 - h_6)$
HE2	$n_C (h_{12} - h_{11}) = X_G (h_6 - h_7)$
T	$W_T = n_C (h_{12} - h_{13})$
MC	$W_{MC} = (1\text{-}x)\, n_C (h_9 - h_8)$
REC	$W_{REC} = x\, n_C (h_{10} - h_{15})$
HTR	$\varepsilon = \frac{T_{13} - T_{14}}{T_{13} - T_{10}}$, $h_{11} - h_{10} = h_{13} - h_{14}$
LTR	$\varepsilon = \frac{T_{14} - T_{15}}{T_{14} - T_9}$ if minimum in hot side
	$\varepsilon = \frac{T_{10} - T_9}{T_{14} - T_9}$ if minimum in cold side
	$(1\text{-}x)(h_{10} - h_9) = h_{14} - h_{15}$
PC	$(1\text{-}x)\, n_C (h_{15} - h_8) = n_W (h_{17} - h_{16})$
η_{Energy}	$\eta = \frac{W_{GT} + W_T - W_C - W_{MC} - W_{REC}}{m_{biomass}LHV_{biomass}}$

3.3. Recuperator effectiveness

The recuperator effectiveness is defined as the ratio of the heat transfer for a real heat exchanger to the maximum heat transferable, where the latter term applies for an ideal heat exchanger with a surface area that is infinite. For a generic heat exchanger, two thermal profile trends result. The hot side has the minimum heat flow capacity if the thermal profiles are divergent, while the cold side has the minimum heat flow capacity if they are convergent [19]. Expressions to model the recuperators are given in Table 3.

3.4. Validation

The present work is simulated and analyzed using Engineering Equation Solver (EES) software. The results are considered acceptable compared to the results provided by Zainal [27] and Alauddin [31] in Table 2, as good agreement is exhibited. All three studies are based on using atmospheric air as the gasification agent and a gasification temperature of 800 °C.

The SCO_2 recompression cycle simulation is based on the study of Wu et al. [32] and, as Fig. 2 depicts, the validated data exhibit acceptable agreement with the results of Wu et al.

4. Results and discussion

To ensure a comprehensive examination of the performance of the system considered, four key parameters are selected for a parametric study: gas turbine inlet temperature (TIT), CO_2 turbine inlet temperature (CTIT), cold-end temperature difference (CETD) for heat exchanger HE1 and topping cycle pressure ratio (r_p). The parametric study also permits an assessment of the optimized parameters. Thermodynamic properties of the system when TIT = 1400 K, $r_p = 7$, CTIT = 645 K and CETD = 245 for HE1 are provided in Table 4.

Fig. 3 demonstrates the effect of r_p on combined cycle energy efficiency for various values of TIT. As shown in this figure, increasing TIT raises the value of energy efficiency. TIT has a considerable impact, mainly because of the dominant increase in gas turbine power output as TIT increases. For a particular r_p value, the system energy efficiency attains a maximum. This particular value of r_p offers the minimum fuel consumption for a fixed output, which decreases environmental emissions, as seen in Fig. 4. Since the total power generated by the system is fixed at 1 MW, the energy efficiency equation presented in Table 3 expresses the maximization of energy efficiency.

Table 4
Values of thermodynamic properties for state points in the system.

State	Temperature (K)	Pressure (kPa)	State	Temperature (K)	Pressure (kPa)
1	298	101.3	10	487	20000
2	557.4	709.3	11	529.1	20000
3	1400	709.3	12	645	20000
4	938	101.3	13	544	7400
5	1522	101.3	14	495	7400
6	802.4	101.3	15	384.5	7400
7	549.1	101.3	16	298	101.3
8	305.2	7400	17	308	101.3
9	366.7	20000			

Fig. 5 shows the cycle energy efficiency variation with CETD of HE1, for fixed values of TIT and r_p. At this particular value of r_p, as we increase the value of CETD, the energy efficiency starts to decrease, which is consistent with studies of other researchers [8,12,33]. This energy efficiency reduction occurs because increasing the value of CETD results in an increase in biomass consumption, as seen in Fig. 6. Since the produced power is fixed, the observed behavior is justified.

Fig. 7 illustrates, for the bottoming cycle, the variation of energy efficiency with CO_2 turbine inlet temperature (CTIT) for several values of gas turbine inlet temperature (TIT). The topping cycle energy efficiency is seen to increase gradually with CTIT until CTIT = 645 K, above which the system energy efficiency decreases as CTIT increases. This behavior can be explained by the variation of biomass flow rate as the CTIT increases. Biomass usage decreases as CTIT increases and reaches a minimum point at CTIT = 645 K and starts to increase beyond this point, which is observed in Fig. 8.

The variations of power production by the topping cycle with CTIT validates the biomass flow rate trend, as described above. The topping

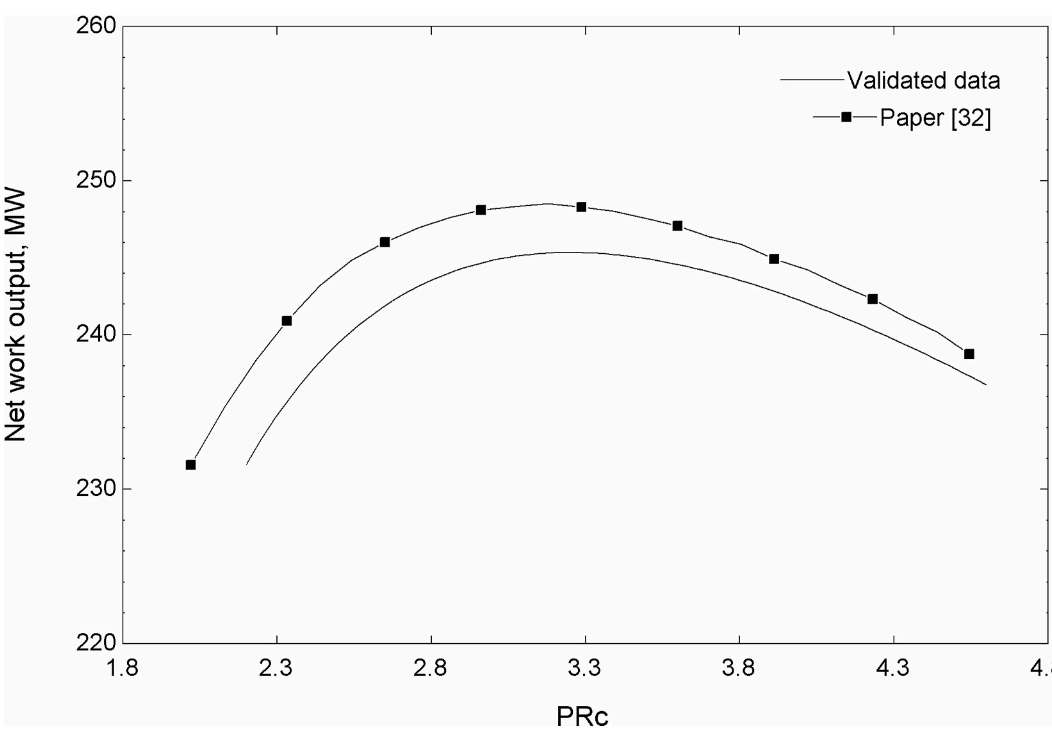

Fig. 2. Comparison of validated data with data from Ref. [32].

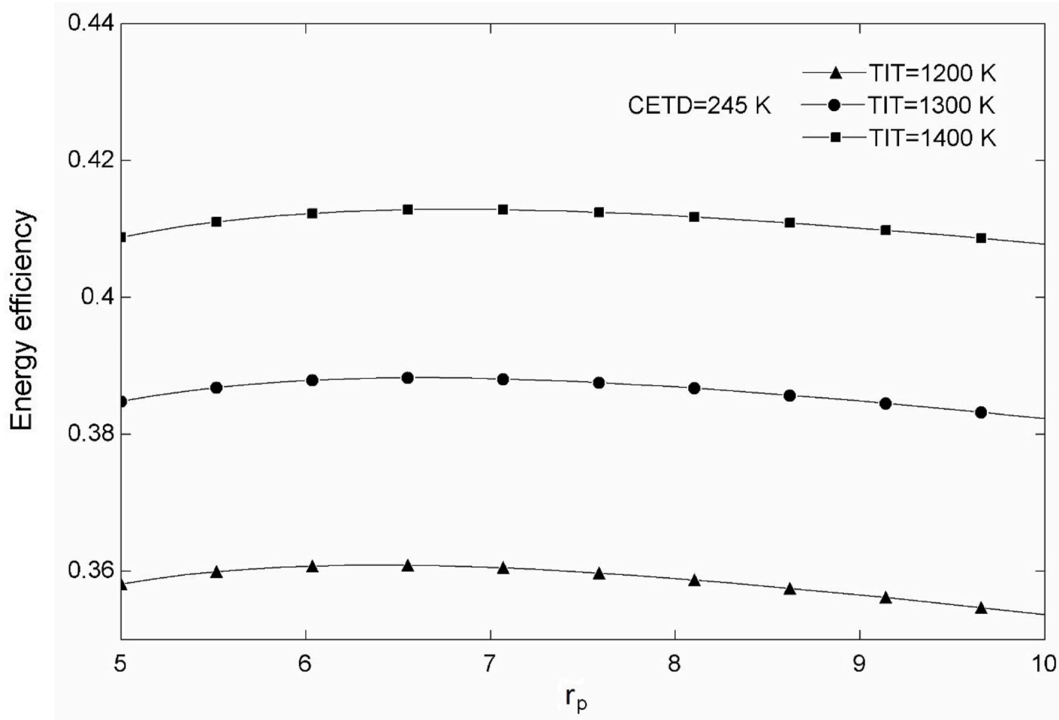

Fig. 3. Variation of energy efficiency for the EFGTRC cycle with pressure ratio (r_p) for several gas turbine inlet temperatures.

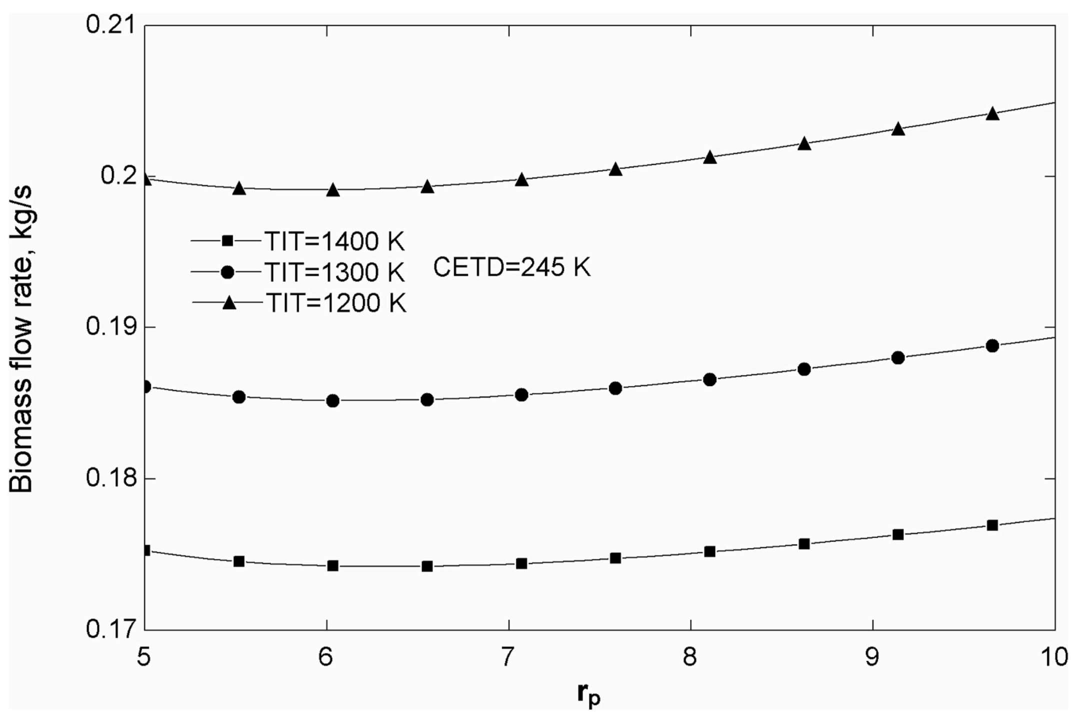

Fig. 4. Variation of biomass flow rate with pressure ratio (r_p) of the EFGTCC cycle for several gas turbine inlet temperatures.

cycle's maximum power output is produced at CTIT = 645 K, as shown in Fig. 9. Considering the fact that biomass usage is a minimum at this point, the topping cycle has a higher share of total power production as total produced power is assumed to be 1 MW. Thus, the maximum waste heat recovery from the second heat exchanger occurs at this point.

Three figures are used to investigate the carbon dioxide emissions of the EFGTRC cycle: Fig. 10a, b and c.

When TIT and CTIT are constant, CO_2 emissions of the EFGTRC reach a maximum at about r_p = 7. When r_p and CTIT are constant, CO_2 emissions decrease gradually as TIT increases. When r_p and TIT are constant, CO_2 emissions reach a maximum at about CTIT = 645 K.

To examine the parameters required for optimum results, we choose three cases to further study system performance. These cases are chosen to be as close as possible to the optimum system parameters and the fixed parameters are: pressure ratio (r_p = 7) and CO_2 turbine inlet temperature (CTIT = 645 K).

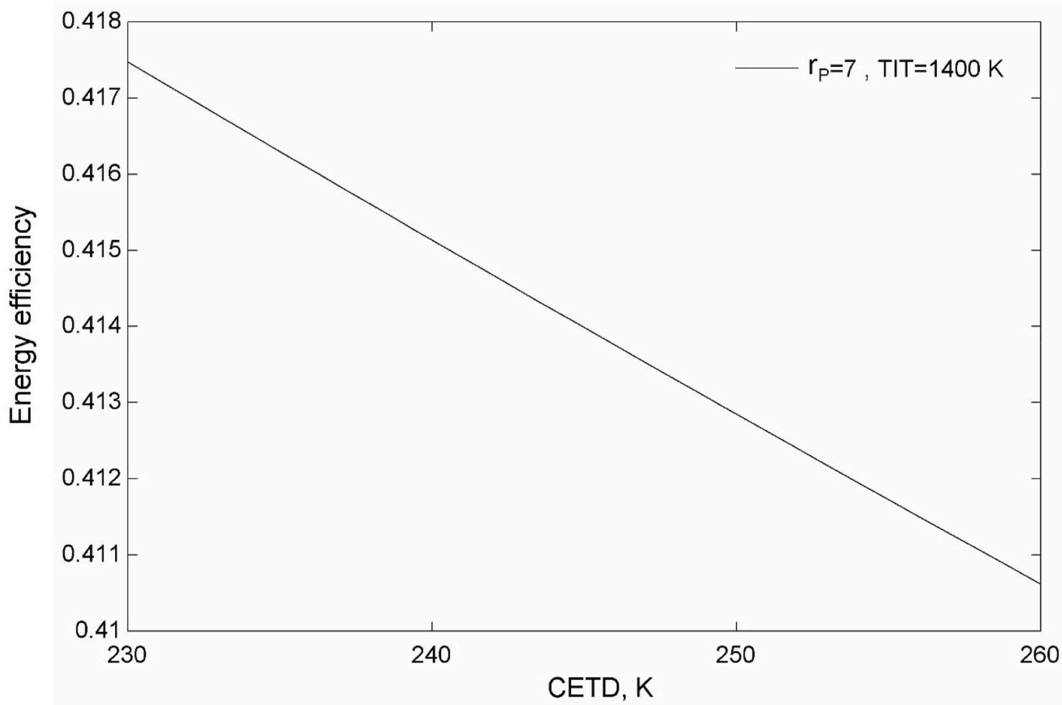

Fig. 5. Variation of energy efficiency for the EFGTRC cycle with cold end temperature difference.

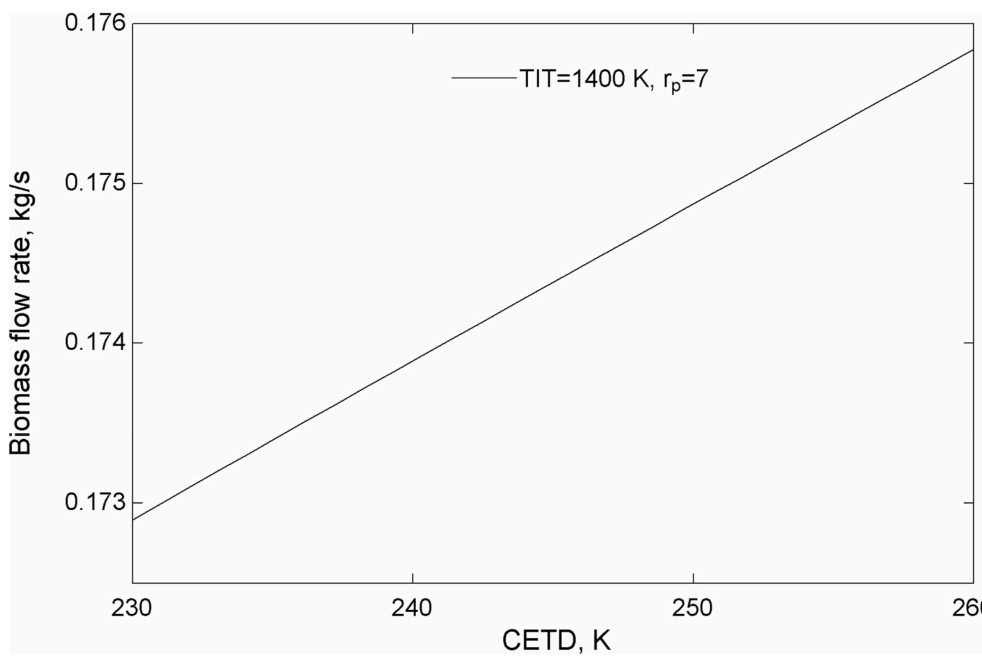

Fig. 6. Variation of biomass flow rate with cold end temperature difference.

Assumptions are given in Table 5 for each case with results. The results in Table 5 provide insights on the impact of the chosen parameters on the size of the system components.

Each case has advantages and disadvantages. Considering the various aspects of the system, case 2 has some clear advantages like the highest energy efficiency and the lowest fuel consumption. The highest overall UA for HE1 is associated with case 2 which indicates that the size of HE1 can be smaller than in the other cases. However, for the same value of LMTD, the overall UA for case 1 is higher than for other cases for HE2. Comparing cases 2 and 3, we can infer that an increase in CETD for heat exchangers reduces the energy efficiency and overall UA, which results in system components being larger [18]. As the components become larger, especially the heat exchangers, their costs rise as well. As the net power output of the system is constant, it is from an economic point of view more advantageous to make the heat exchangers smaller to avoid unnecessary extra expenses.

Note that throughout this paper we consider CETD for HE2 to be constant (20 K). Increasing this value, just like HE1, leads to a reduction in the value of overall UA.

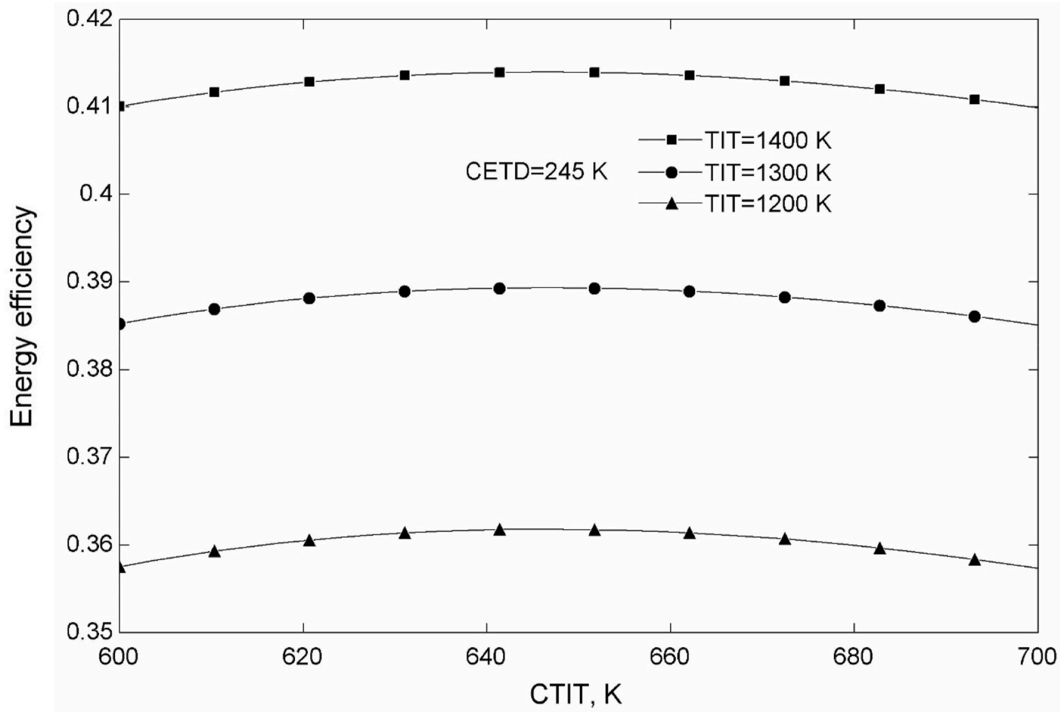

Fig. 7. Variation of energy efficiency with CO_2 turbine inlet temperature for several values of gas turbine inlet temperature.

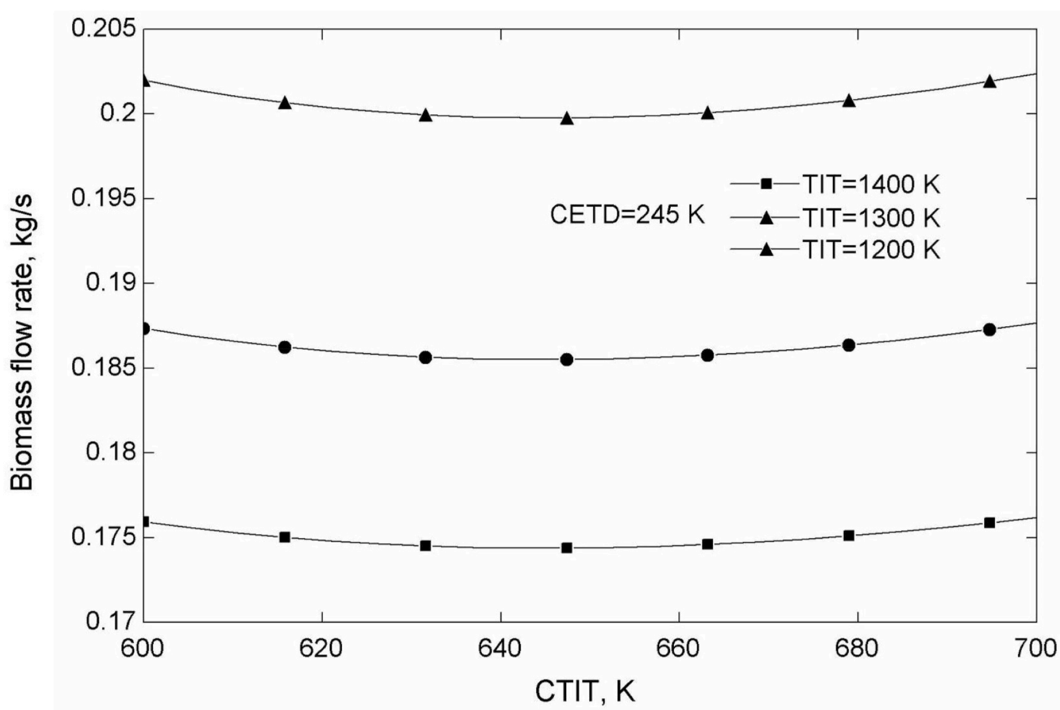

Fig. 8. Variation of biomass flow rate with CO_2 turbine inlet temperature for several values of gas turbine inlet temperature.

5. Conclusion

An externally fired gas turbine coupled with a partial cooling SCO_2 power system integrated with a biomass gasification plant using wood as fuel is proposed and examined. It is shown that, at certain values of r_p and CTIT, we achieve the maximum value of energy efficiency for the system. At these particular values, an increase in the value of TIT boosts the energy efficiency; contrarily an increase in the value of CETD has a negative effect on system energy efficiency. Additionally, with due attention to energy efficiency and fuel consumption, case 2 with variable parameters of TIT = 1400 K and CETD = 245 K offers more favorable performance compared to other cases. However, from an economic point of view considering capital investment and maintenance expenses, case 3 (TIT = 1400 K, CETD = 275 K) is favorable because the value of overall UA is lower for this case, which means the component is smaller. Case 1 (TIT = 1200 K, CETD = 245 K) performs worse than the other

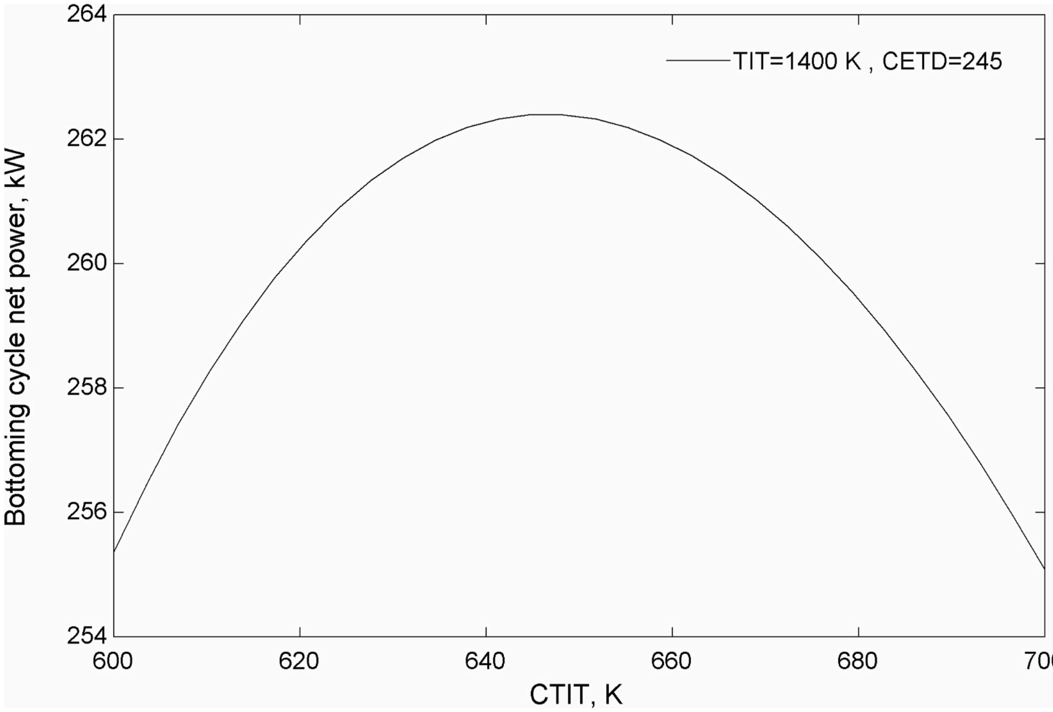

Fig. 9. Variation of topping cycle net power with CO_2 turbine inlet temperature.

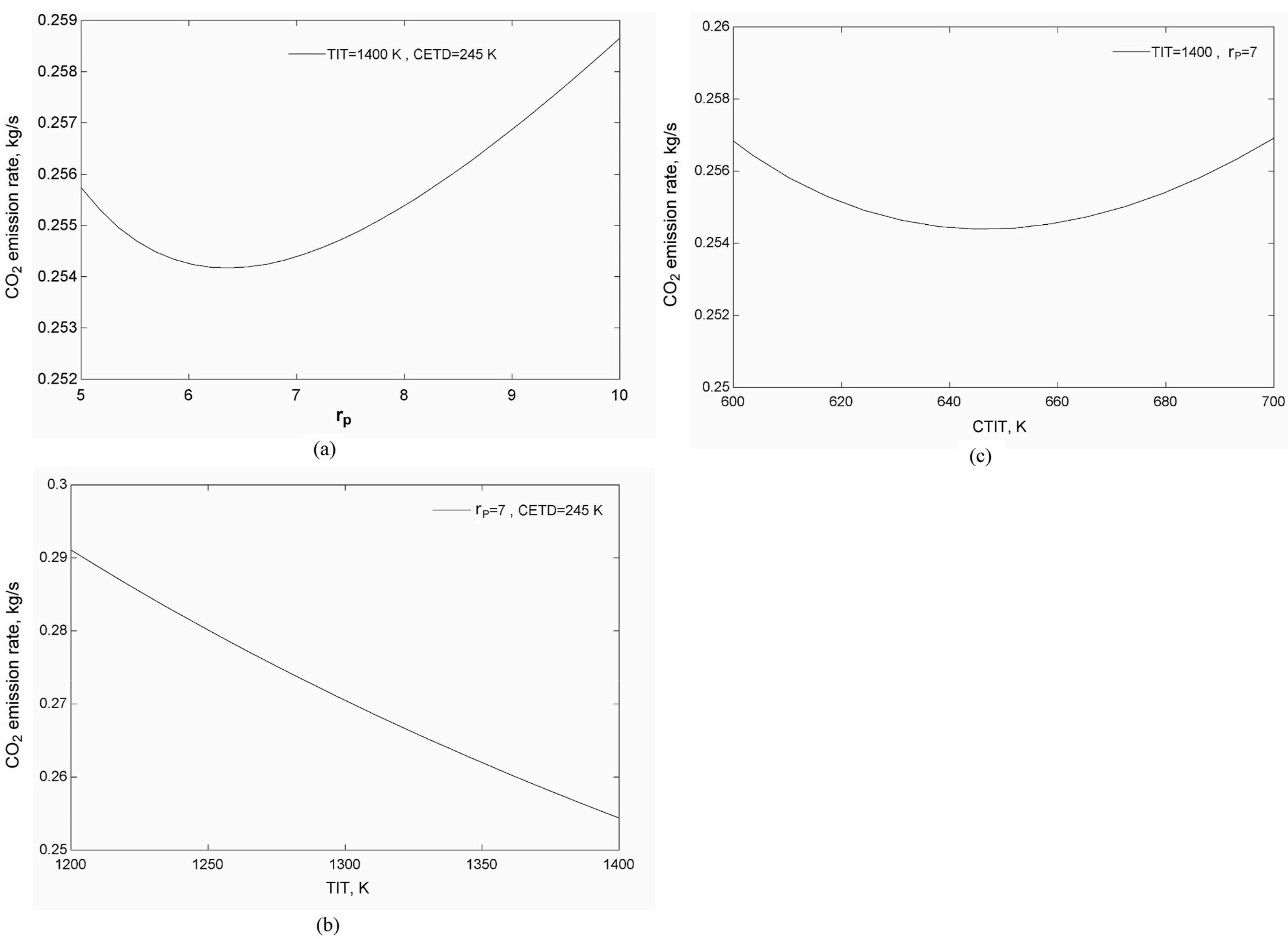

Fig. 10. Variation of CO_2 emission rate with a) pressure ratio (r_p), b) gas turbine inlet temperature, c) CO_2 turbine inlet temperature.

Table 5
Comparison of three possible cases for a biomass fired EFGTRC power plant having a 1 MW net power output.

Parameter	Case 1 TIT = 1200 K CETD HE1 = 245 K	Case 2 TIT = 1400 K CETD HE1 = 245 K	Case 3 TIT = 1400 K CETD HE1 = 275 K
Mass flow rate (kg/s)			
Biomass	0.1999	0.1745	0.1774
Air	3.447	2.688	2.601
CO_2	7.475	5.962	6.518
Energy efficiency (%)	0.3559	0.4118	0.4051
Heat rate (kW)			
HE1	2480	2576	2492
HE2	1008	788.9	854.8
Temperature difference (K)			
$LMTD_{HE1}$	200.6	176.4	207.5
$LMTD_{HE2}$	53.48	53.48	58.58
Overall UA (kW/K)			
UA_{HE1}	12.36	14.61	12.41
UA_{HE2}	18.85	14.75	14.12

cases both thermodynamically and economically. The value of x at the recompression cycle for case 2 is 0.3803.

CRediT authorship contribution statement

Shayan Sharafi laleh: Conceptualization, Data curation, Formal analysis, Investigation, Methodology, Resources, Software, Validation, Writing – original draft, Writing – review & editing. **Seyed Hamed Fatemi Alavi:** Conceptualization, Data curation, Formal analysis, Investigation, Methodology, Project administration, Resources, Software, Validation, Writing – original draft, Writing – review & editing. **Saeed Soltani:** Conceptualization, Data curation, Formal analysis, Investigation, Methodology, Project administration, Resources, Software, Supervision, Validation, Writing – original draft, Writing – review & editing. **S.M.S. Mahmoudi:** Conceptualization, Data curation, Formal analysis, Investigation, Methodology, Project administration, Resources, Software, Supervision, Validation, Writing – original draft, Writing – review & editing. **Marc A. Rosen:** Conceptualization, Data curation, Formal analysis, Investigation, Methodology, Project administration, Resources, Software, Supervision, Validation, Writing – original draft, Writing – review & editing.

Declaration of competing interest

The authors declare that they have no known competing financial interests or personal relationships that could have appeared to influence the work reported in this paper.

References

[1] E. Agbor, A.O. Oyedun, X. Zhang, A. Kumar, Integrated techno-economic and environmental assessments of sixty scenarios for co-firing biomass with coal and natural gas, Appl. Energy 169 (2016) 433–449.
[2] B. Knight, A. Westwood, World biomass review: biomass as a global power source, Refocus 5 (2004) 42–44.
[3] E. Toklu, Biomass energy potential and utilization in Turkey, Renew. Energy 107 (2017) 235–244.
[4] N. Cooper, A. Panteli, N. Shah, Linear estimators of biomass yield maps for improved biomass supply chain optimization, Appl. Energy 253 (2019), 113526.
[5] J.M. Beer, Combustion technology developments in power generation in response to environmental challenges, Prog. Energy Combust. Sci. 26 (2000) 301–327.
[6] Y. Sanjay, O. Singh, B.N. Prasad, Energy and exergy analysis of steam cooled reheat gas steam combined cycle, Appl. Therm. Eng. 27 (2007) 2779–2790.
[7] S.B. Ferreira, P. Pilidis, Comparison of externally fired and internal combustion gas turbines using biomass fuel, ASME J Energy Resource Technology 123 (2001) 291–296.
[8] A. Datta, R. Ganguly, L. Sarkar, Energy and exergy analyses of an externally fired gas turbine (EFGT) cycle integrated with biomass gasifier for distributed power generation, Energy 35 (2010) 341–350.
[9] M. Mehrpooya, M. Khalili, M.M. Moftakhari Sharifzadeh, Model development and energy and exergy analysis of the biomass gasification process (Based on the various biomass sources), Renew. Sustain. Energy Rev. 91 (2018) 869–887.
[10] P. McKendry, Energy production from biomass (parts 1–3), Bioresour. Technol. 83 (2002) 37–63.
[11] A.V. Bridgewater, A.J. Toft, J.G. Brammer, A techno-economic comparison of power production by biomass fast pyrolysis with gasification and combustion, Renew. Sustain. Energy Rev. 6 (2002) 181–248.
[12] D. Vera, F. Jurado, J. Carpio, Study of a downdraft gasifier and externally fired gas turbine for olive industry wastes, Fuel Process. Technol. 92 (2011) 1970–1979.
[13] S.M. Camporeale, A.M. Pantaleo, P.D. Ciliberti, B. Fortunato, Cycle configuration analysis and techno-economic sensitivity of biomass externally fired gas turbine with bottoming ORC, Energy Convers. Manag. 105 (2015) 1239–1250.
[14] S. Cordiner, V. Mulone, Experimental-numerical analysis of a biomass fueled microgeneration power-plant based on microturbine, Appl. Therm. Eng. 71 (2014) 905–912.
[15] I.W. Eames, K. Evans, S. Pickering, A comparative study of open and closed heat engines for small scale CHP applications, Energies 9 (2016) 130.
[16] M. Kautz, U. Hansen, The externally fired gas turbine (EFGT-cycle) for decentralized use of biomass, Appl. Energy 84 (2007) 795–805.
[17] Q. Liu, Z. Bai, X. Wang, J. Lei, H. Jin, Investigation of thermodynamic performances for two solar-biomass hybrid combined cycle power generation systems, Energy Convers. Manag. 122 (2016) 252–262.
[18] S. Soltani, S.M.S. Mahmoudi, M. Yari, M.A. Rosen, Thermodynamic analyses of an externally fired gas turbine combined cycle integrated with a biomass gasification plant, Energy Convers. Manag. 70 (2013) 107–115.
[19] G. Manente, F.M. Fortuna, Supercritical CO2 power cycles for waste heat recovery: a systematic comparison between traditional and novel layouts with dual expansion, Energy Convers. Manag. 197 (2019), 111777.
[20] C. Laux, A. Gotter, F. Eckert, M. Neef, Experimental results of a low-pressure steam Rankine cycle with a novel water lubricated radial inflow turbine for the waste heat utilization of internal combustion engines, Energy Convers. Manag. 271 (2022), 116265.
[21] D. Lou, D. Huang, Thermodynamic and exergoeconomic investigation of various SCO2 Brayton cycles for next generation nuclear reactors, Energy Convers. Manag. 209 (2020), 112649.
[22] E.P. Reznicek, T. Neises, R.J. Braun, Optimization and techno-economic comparison of regenerators and recuperators in sCO2 recompression Brayton cycles for concentrating solar power applications, Sol. Energy 238 (2022) 327–340.
[23] Y. Khan, R. Shyam Mishra, Performance analysis of solar driven combined recompression main compressor intercooling supercritical CO2 cycle and organic Rankine cycle using low GWP fluids, Energy and Built Environment 3 (2022) 496–507.
[24] A. Bhattacharya, D. Manna, B. Paul, A. Datta, Biomass integrated gasification combined cycle power generation with supplementary biomass firing: energy and exergy based performance analysis, Energy 36 (2011) 2599–2610.
[25] A. Issakhov, Y. Zhandaulet, Thermal pollution zones on the aquatic environment from the coastal power plant: numerical study, Case Stud. Therm. Eng. 25 (2021), 100901.
[26] A.D. Akbari, S.M.S. Mahmoudi, Thermoeconomic analysis & optimization of the combined supercritical CO2 (carbon dioxide) recompression Brayton/organic Rankine cycle, Energy 78 (2014) 501–512.
[27] Z.A. Zainal, R. Ali, C.H. Lean, Prediction of performance of downdraft gasifier using equilibrium modeling for different biomass materials, Energy Convers. Manag. 42 (2001) 1499–1515.
[28] A. Kushwah, T.R. Reina, M. Short, Modelling approaches for biomass gasifiers: a comprehensive overview, Sci. Total Environ. 834 (2022), 155243.
[29] A. Ibrahim, S. Veremieiev, P.H. Gaskell, An advanced, comprehensive thermochemical equilibrium model of a downdraft biomass gasifier, Renew. Energy 194 (2022) 912–925.
[30] S. Jarungthammachote, A. Dutta, Thermodynamic equilibrium model and second law analysis of a downdraft waste gasifier, Energy 32 (2007) 1660–1669.
[31] Z.A. Alauddin, Performance and Characteristics of a Biomass Gasifier System, University of Wales, College of Cardiff, UK, 1996. PhD thesis.
[32] C. Wu, S. Wang, X. Feng, J. Li, Energy, exergy and exergoeconomic analyses of a combined supercritical CO2 recompression Brayton/absorption refrigeration cycle, Energy Convers. Manag. 148 (2017) 360–377.
[33] D. Vera, F. Jurado, B. Mena, G. Schories, Comparison between externally fired gas turbine and gasifier–gas turbine system for the olive oil industry, Energy 36 (2011) 6720–6730.